Westinghouse
Electric Corporation

Energy Systems

Box 355
Pittsburgh Pennsylvania 15230-0355

NSD-NRC-96-4912
DCP/NRC0682
Docket No.: STN-52-003

December 12, 1996

Document Control Desk
U.S. Nuclear Regulatory Commission
Washington, D. C., 20555

ATTENTION: T. R. QUAY

SUBJECT: AP600 EX-VESSEL SEVERE ACCIDENT PHENOMENA (DRAFT PRA APPENDIX B)

Dear Mr. Quay:

Enclosed is a draft copy of AP600 Probabilistic Risk Assessment (PRA) Appendix B. This appendix provides the results of the deterministic evaluations of the consequences of ex-vessel severe accident phenomena for the AP600 design.

PRA Appendix B closes, from a Westinghouse perspective, the following DSER open items: 19.2.3.3-3, 19.2.3.3-4, 19.2.3.3-6, and 19.2.3.3-7. The NRC technical staff should review this enclosure. The status of these open items will be changed to "Action N" in the OITS on January 2, 1997.

Appendix B will be included in the next revision to the PRA. No changes are expected between the draft copy enclosed with this letter and the Appendix B that will be included in the next PRA revision. If there are any changes, they will be clearly identified to the staff.

Please contact Cynthia L. Haag on (412) 374-4277 if you have any questions concerning this transmittal.

Brian A. McIntyre

Brian A. McIntyre, Manager
Advanced Plant Safety and Licensing

1/1
E004

Enclosure

cc: J. Sebrosky, NRC (enclosure)
J. Kudrick, NRC (w/o enclosure)
N. J. Liparulo, Westinghouse (w/o enclosure)

3022A

Enclosure to Westinghouse
Letter NSD-NRC-96-4912

December 12, 1996

APPENDIX B

EX-VESSEL SEVERE ACCIDENT PHENOMENA

One of the key AP600 severe accident design features is the capability to retain the core debris within the reactor vessel for a large number of severe accident sequences by flooding the reactor cavity and submerging the outer surface of the reactor vessel. The heat removal capability of the water on the external surface of the reactor vessel prevents the reactor vessel wall from reaching temperatures where failure of the reactor vessel could occur. This has been termed in-vessel retention and is described in detail is other sections of the AP600 Level 2 PRA. The primary benefit of in-vessel retention of the core is that ex-vessel severe accident phenomena associated with relocation of core debris to the containment, which can be a dominant containment failure mechanism, are physically prevented. Thus, retention of the core within the reactor vessel results in a significant reduction in the potential for significant fission product releases to the environment for core damage accidents.

The probability of various levels of fission product releases (release categories) has been determined in the AP600 Level 2 PRA, using a containment event tree which describes the various severe accident phenomena that can impact the fission product release quantities and probability of release. In the quantification of the AP600 Level 2 PRA it was conservatively assumed that the containment would fail at the time of reactor vessel failure for all core damage sequences in which the core debris could not be retained within the reactor vessel. The two principle ways identified in the Level 2 PRA of retaining the core within the reactor vessel are reflooding the core with water before the core begins to relocate within the reactor vessel and submerging the outer surface of the reactor vessel to the reactor coolant loop nozzles. Using this conservative approach, the regulatory and industry severe accident performance targets for the AP600 design criteria were met. Therefore, it was considered unnecessary to investigate the consequences of reactor vessel failure on a realistic basis, including quantification of uncertainties.

The purpose of this section is to provide the results of a limited number of deterministic investigations of the consequences of ex-vessel severe accident phenomena for the AP600 design. The results of these deterministic investigations show that the challenges to the integrity of the containment posed by ex-vessel severe accident phenomena are generally within the structural capability of the containment. From these investigations, the conclusion is the capability to prevent large fission product releases to the environment does not depend on the ability to retain the core within the reactor vessel for core damage accident sequences.

The AP600 design includes features to enhance the likelihood of retaining the core within the reactor vessel for severe accident sequences. These features include:

- Depressurization of the reactor coolant system (RCS) in the event of an accident by either automatic or manual actuation of the automatic depressurization system (ADS)

- A containment layout wherein the water relieved from the reactor coolant system (either from the ADS discharge or a break in the RCS) would accumulate in the reactor cavity region

- The capability to manually initiate flooding of the reactor cavity by gravity draining the in-containment refueling water storage tank (IRWST) into the reactor cavity

- The absence of in-core penetrations in the reactor vessel bottom head eliminates a possible reactor vessel failure mode

- The reactor cavity layout provides for rapid flooding of the reactor vessel to the reactor coolant loop nozzle elevation

- The unique reactor vessel insulation design assures the ingress of water to the region between the insulation and the reactor vessel and the egress of steam from that same region to promote cooling of the external surface of the reactor vessel.

Some of the AP600 design features to reduce the probability of a core damage accident and to enhance the likelihood of in-vessel retention of core debris in the event of a core damage accident are counter to the design philosophy that would be used to mitigate the consequences of ex-vessel severe accident phenomena. In particular, two of the design features are mutually exclusive between preventing ex-vessel phenomena and mitigating the consequences of ex-vessel phenomena. On the balance, the AP600 severe accident risk profile is substantially reduced by the features that prevent ex-vessel severe accident phenomena. Two of the more noteworthy features are:

- The large mass and low power density of the AP600 core provides for a much slower accident progression which enhances the capability to prevent a core damage accident (i.e., a reduced core damage frequency). The larger mass of core materials may result in more severe consequences from some of the potential ex-vessel phenomena such as core debris coolability, direct containment heating and core concrete interactions.

- The small reactor cavity floor area reduces the amount of water required to completely submerge the reactor vessel. The small cavity floor area also provides for a more rapid flooding of the cavity if manual initiation of IRWST draining to the reactor cavity is required to submerge the reactor vessel. The small reactor cavity floor area may result in more severe consequences from some of the severe accident ex-vessel phenomena such as core debris coolability and core concrete interactions.

The limited deterministic investigations of ex-vessel severe accident phenomena described in this section includes: ex-vessel steam explosions, direct containment heating and core concrete interactions. These ex-vessel phenomena are strongly dependent on the assumptions made concerning the mode of reactor vessel failure for the AP600 design. Therefore, the reactor vessel failure mode is described first, followed by a description of the ex-vessel phenomena investigations.

B.1 Reactor Vessel Failure

The AP600 reactor vessel has a main cylindrical section approximately 4 meters in diameter and a hemispherical bottom head with a radius of approximately 2 meters. The bottom head is approximately 15 cm (6 inches) in thickness and is made of carbon steel with an inner cladding of stainless steel to prevent contact between reactor coolant and carbon steel during normal plant operations. The bottom head of the reactor vessel does not contain any discontinuities or penetrations that could impact the mode of reactor vessel failure as the moiten core material relocates to the bottom head.

Based on investigations of the possible failure modes for the AP600 reactor vessel, as documented in reference B-1, the most likely failure mode is creep failure of the vessel wall due to heating of the vessel wall by the core debris that has relocated to the reactor vessel bottom head. Since creep failure is a strongly temperature-dependent phenomena, the location of the failure is predicted to be at the upper surface of the core debris pool that has relocated to the reactor vessel bottom head. For most severe accident sequences, this location is near the junction of the hemispherical bottom head and the cylindrical portion of the vessel.

As described in reference B-2, the presence of water on the external surface of the reactor vessel, as in the case of a flooded reactor cavity, does not alter the conclusion that the highest heat fluxes to the reactor vessel walls will be at a point near the top of the in-vessel molten core pool. This would correspond to the region of the reactor vessel most susceptible to creep failure. However, as described in reference B-2, the failure of the reactor vessel for the case in which the reactor coolant system is depressurized and the reactor cavity is filled with water to the reactor coolant loop elevation is physically unreasonable. Even considering the uncertainties related to in-vessel retention of core debris for these case, the potential for vessel failure is physically unreasonable.

For the case in which the outside of the reactor vessel is initially submerged but a sufficient in-flow of water to the reactor cavity cannot be maintained, the reactor vessel wall location experiencing the highest heat fluxes would uncover and lose its external cooling before other locations on the reactor vessel lower head. Thus, creep failure of the vessel would be expected to occur at the same location as the case with no water in the reactor cavity.

Two reactor vessel creep failure cases, as described below, are carried through the deterministic analyses of ex-vessel steam explosions and core concrete interactions. However, in the case of direct containment heating, a failure of the reactor vessel at an elevation at or above the surface of the core debris in the reactor vessel would result in only a small fraction of the total core debris being transported from the reactor vessel. With only a small fraction of the core debris transported to the containment, direct containment heating does not represent a challenge to the integrity of the containment. Thus, the deterministic analysis of direct containment heating considers an undefined reactor vessel failure near the bottom of the vessel bottom head such that all of the core debris that has relocated to the bottom head

at the time of vessel failure will be expelled from the reactor vessel into the reactor cavity before the discharge of reactor coolant system gases into the cavity.

For the consideration of ex-vessel steam explosions and core-concrete interactions, it is assumed that the reactor vessel is initially submerged in water but that gravity draining of water from the IRWST does not occur. In this case, the heat removed from the reactor vessel by the water in the reactor cavity results in a boil-down of the water in the cavity. The steam produced by the boiling is condensed by the containment heat sinks and returned to the IRWST and the refueling canal where it is held-up and cannot return to the cavity. As the water in the reactor cavity boils down, the outside of the reactor vessel at the elevation at the top of the in-vessel core pool will dry-out and begin to heat up. As the vessel wall heats up, it undergoes thinning due to dissolution and melting until failure occurs. The manner in which the reactor vessel fails is treated in two separate cases described below.

In the first case, the formation of a localized opening occurs due to asymmetric heating around the circumference followed by the vessel tearing around nearly all of its circumference. This would result in the bottom part of the reactor vessel and the bottom head hinging such that the lower head swings downward and comes to rest on the cavity floor. This behavior is illustrated in Figure B-1. A hinging type of failure would result in an immediate pouring of core debris onto the cavity floor with metal flowing ahead of oxide. The relationship between the height of the reactor vessel above the floor is such that all but a minor part of the oxide melt would be free to flow immediately out of the head.

In the second case, the head and bottom part of the vessel do not hinge downward. In this case, the formation of a localized opening permits molten core debris to drain into the cavity lowering the in-vessel core debris depth and thereby decreasing the thermal load on the vessel wall formerly adjacent to the melt. This type of failure is illustrated in Figure B-2. In this case, the continued boildown of water level is followed by the release of the core debris located above the water level after a delay interval during which heatup, thinning, and localized failure of the wall will occur. Over time, the elevation of the failure location moves downward over the vessel wall and lower head. This type of failure gives rise to a very slow release rate with the core debris first relocating downward through the water before collecting and spreading on the cavity floor.

For both mechanistic reactor vessel failure cases, the condition of the core debris inside the reactor vessel at the time of vessel failure is defined in Table B-1.

B.2 Direct Containment Heating

Direct Containment Heating (DCH) is defined as the rapid energy addition to the containment atmosphere as a result of several physical and chemical processes that can occur if the core debris is forcibly ejected from the reactor vessel. The prerequisites for direct containment heating are vessel failure occurs at a location where a substantial portion of the core debris that has relocated to the lower head is ejected into the reactor cavity before the RCS gases are discharged from the RCS and that the RCS is at a high pressure (sometimes called high

pressure melt ejection or HPME). Under these conditions, it is postulated that the molten core debris on the reactor cavity floor will be swept out of the reactor cavity with the gases that are discharged from the reactor cavity. The airborne, fragmented core debris then rapidly transfers its sensible heat to the containment atmosphere in one of the containment compartments, as dictated by the gas flow from the reactor cavity. In addition to transfer of sensible heat, the unoxidized metal in the core debris can undergo an exothermic oxidation reaction in the presence of the oxygen in the containment compartment. This heat is also added to the containment atmosphere in that compartment. Finally, if the flammable gases in that containment compartment (including the added flammable gases from the oxidation reactions in that compartment) are ignited, the heat of combustion will be added to the containment atmosphere gases in that compartment. Experimental evidence (reference B-3) shows that containment compartmentalization and the flow paths from the reactor cavity to each compartment have a strong effect on the containment conditions that can result from a high pressure melt ejection. A screening model for predicting the potential impact of direct containment heating on the containment integrity was developed from the experimental considerations (reference B-4).

The Pilch 2-Cell model presented in reference B-4 was used to determine the potential impact of the direct containment heating on the integrity of the containment for the AP600 design. The input parameters for the model, presented in Table B-2, are based on the AP600 reactor cavity and containment design. The area above the operating deck is modelled as one cell and the steam generator compartments are modelled as the second cell. Various dead-end volumes are not included in the 2-cell model since their vapor space would not be easily accessible for energy transfer from core debris ejected from the reactor cavity. For the AP600 design, the possible flow paths for core debris transported from the reactor cavity are the area around the reactor vessel flange which communicates directly with the upper containment volume (the volume above the operating deck). There are two flow paths from the cavity to the steam generator compartments: 1) the area where the coolant loops penetrate through the biological shield, and 2) a ventilation shaft from the roof of the reactor coolant drain tank room that Tee's to a common tunnel between the two steam generator compartments. For the purposes of applying the Pilch 2-Cell model to the AP600 configuration, the two steam generator compartments were modelled as one compartment since the compartment volumes and flow areas are nearly identical for each steam generator compartment. Also in this deterministic assessment of DCH, the reactor vessel was assumed to fail at the bottom of the hemispherical head to maximize the amount of core debris that would be forcibly ejected from the reactor vessel prior to the discharge of high pressure gases from the vessel. It was assumed that 50 percent of the total UO_2 and Zr in the core would be forcibly ejected from the vessel at vessel failure. In addition, it was conservatively assumed that 90 percent of the Zr was unoxidized during the in-vessel core heatup and relocation phase of the accident.

The application of the Pilch 2-Cell model to the AP600 design leads to the conclusion that direct containment heating would not challenge the integrity of the containment. The results of the bounding analysis show a pressure increase of 46.4 psia (0.32 MPa). Based on an initial containment pressure of 45 psia (0.31 MPa), this yields a final pressure of 91.4 psia (0.63 MPa), which is well below the point where containment failures are predicted to occur.

B.3 Ex-Vessel Steam Explosions

B.3.1 Ex-Vessel Steam Explosion Loads

If the reactor vessel fails and the molten core debris exiting the vessel contacts water in the reactor cavity, there is the potential for a steam explosion. To estimate the maximum upper bound impact of an ex-vessel steam explosion on the integrity of the AP600 containment, analyses were performed using the TEXAS computer code (reference B-5).

The input for the TEXAS analyses were derived from the two reactor vessel failure cases described previously. The key input parameters are given in Table B-3. The elevation of the water is assumed to be at the elevation of the vessel failure location to give the deepest possible water pool and thus the worst case scenario. It was assumed that only the initial pour of molten metal is important in the analyses since the initial interaction between the water and the debris is most important. The fuel coolant interaction is assumed to trigger at the time that the debris comes in contact with the cavity wall or floor. Any debris that enters the pool after the time of the triggering event is not considered in the analysis.

Since the TEXAS code is a one-dimensional model, two different water pool depths were used to represent possible trigger locations at the cavity floor and the cavity walls. A water depth of 12.8 feet (3.89 meters) represents the case where the explosion is triggered when the core debris contacts the floor. This is the initial water depth from the cavity floor to the vessel failure location at the top of the debris pool. A water depth of 18.1 inches (0.46 meters) is used to represent the case where the explosion triggers when the debris contacts the cavity walls. This is the distance between the cavity walls and the reactor vessel.

For the hinged vessel failure mode, the TEXAS code was first run to find the time at which debris comes into contact with the cavity floor or walls. This was calculated to be 1 second for the floor and 0.5 seconds for the wall. Using these trigger times, a peak pressure was calculated for deep and shallow pools of 24,700 psi (170 MPa) and 4350 psi (30 MPa) respectively. For the deep water pool, the peak pressure occurs at 7.4 feet (2.25 meter) from the bottom of the pool at 3.5 milliseconds after the explosion trigger. For the case of the shallow water pool, the peak pressure occurs at 0.82 feet (0.25 meters) from the bottom of the cavity at 3 milliseconds after the explosion trigger. This translates to a peak impulse loading of 71 psi-seconds (490 kPa-seconds) for the deep pool and 9.57 psi-seconds (66 kPa-seconds) for the shallow pool. These peak impulse loadings occur in the pool and are significantly diminished by distance.

The localized failure case has a much slower debris pour and a trigger time of 5 and 0.5 seconds was used for deep and shallow water pools respectively. This trigger time was set to the time at which debris came into contact with the cavity wall of floor as determined by the TEXAS code mixing calculation. The peak pressure of 87 psi (0.6 MPa) for the deep pool and 23 psi (0.16 MPa) for the shallow pool are substantially lower than in the hinged reactor vessel failure case described above. For this vessel failure mode, there is a significantly slower debris flow rate which results in much less debris mass and energy to

interact with the water pool. The corresponding peak impulse loadings for the deep pool was 3 psi-seconds (2.1 kPa-second) at a distance of about 1.5 feet (0.5 meters) from the bottom of the pool. In the shallow pool case, there was essentially no steam explosion and thus peak impulse loadings are negligible.

Several sensitivity analyses were performed to determine the impact of varying key parameters that could affect the consequences of a steam explosion. The results of these sensitivities are presented in Table B-4. While the sensitivity analyses point out that the code user can control the results by the choice of input parameters, the analysis results described above represent very conservative bounding values for an ex-vessel steam explosion in the AP600 reactor cavity.

B.3.2 Structural Response to Steam Explosions

An evaluation of the structural integrity of the reactor vessel cavity concrete structure, and the response behavior of the reactor pressure vessel subjected to the defined ex-vessel steam explosion loadings was performed. The ex-vessel steam explosion scenarios are of short time duration impulsive loadings and therefore, the dynamic response characteristics of the structures and the reactor vessel must be considered.

B.3.2.1 Assessment of the Reactor Cavity Concrete and Steel Structures

The interior concrete structures in the vicinity of the reactor cavity were analyzed for the dynamic impulsive loading associated with a hinged reactor vessel failure mode. The analysis considered the reactor cavity floor and the wall to be equivalent one-degree of freedom dynamic systems. The structures were modelled as plates following classical plate theory for deflections in the elastic range. The shape of the loading function was idealized conservatively as a triangular pulse loading of time durations that can range between 0.004 and 0.006 second. Equivalent static analyses were performed to assess the structural integrity of the floor and walls. For equivalent static analyses, a dynamic load factor of 1.5 was used. This factor is the maximum value for any ratio of impulse duration and system period. It is conservative since it represents system frequencies above 100 hertz. Lower dynamic amplification factors will exist for lower frequencies. Therefore, this factor is conservative since the structural frequency of the wall or floor will be lower. Material strength of 60 ksi (413 MPa) for the rebar, and 4000 psi (27.6 MPa) for the compressive strength of concrete was used in the assessment. Failure due to gross structural failure or punching shear was investigated.

For the floor structure, the steam explosion resulting from the hinged reactor vessel failure, as calculated by the TEXAS code, gives a peak impulse loading of approximately 24,700 psi (170 MPa). With a dynamic loading factor of 1.5 applied uniformly over the entire floor of the reactor cavity, this is equivalent to 37,050 psi (255 MPa). The reactor cavity floor was conservatively modelled as a square reinforced concrete slab that is 17 feet (5.18 meters) on edge and 11 feet (3.35 meters) thick fixed on all edges. The reactor cavity floor is split by

the containment vessel into two portions with 5 feet (1.5 meters) or less above the vessel, and 6 feet (1.8 meters) or more below.

For the side reactor cavity wall, the steam explosion load resulting from the hinged reactor vessel failure, as calculated by the TEXAS code, gives a peak impulse loading of approximately 4350 psi (30 MPa). With a dynamic loading factor of 1.5 uniformly over the side wall, this is equivalent to 6538 psi (45 MPa). The most critical wall in the reactor vessel cavity is about 36 inches (~1 meter) thick, and is conservatively assumed fixed at three edges and simply supported on the fourth edge.

The dynamic impulse loadings associated with the localized mode of reactor vessel failure are enveloped by the hinged failure loadings.

It was determined that both the floor and wall structures will not retain their structural integrity with loading associated with hinged vessel failure ex-vessel steam explosion loading. Failure of the wall will not impair the overall structural integrity of the interior concrete structure. To determine the effect of the loss of the floor structure on safety function (leakage of radioactivity into the atmosphere) an evaluation of the structural integrity of the containment vessel was made.

To assess whether the containment would retain its leak tightness with failure of floor and wall structures, time history analyses were performed using the triangular pulse loading and equivalent one-degree of freedom dynamic model. The mass associated with the response is the portion of the concrete floor that is defined to fail. The stiffness is that associated with the soil. The range of soil stiffness associated with the AP600 project was used. It was determined that largest response was that associated with the lowest stiffness soil case (soft to medium soil, 520 k/cubic-foot, which is 81 MegaNewtons/cubic-meter). The amount of deflection (maximum value less than 6 inches, which is 15 cm) associated with failed concrete was used to define the potential strain in the containment vessel. The strain or elongation is defined as the ratio of the deflection divided by the associated length of the containment vessel steel subjected to the pulling tension. A 13 foot (4 meter length) was used for the containment vessel steel. It is the minimum length that could experience this tensile strain. It is noted that the containment vessel is not "bonded" (attached structurally) to the concrete, and therefore, it is free to slide between the two concrete layers. Therefore, the length used for the containment vessel is conservative since it produces an upper bound strain level. It was determined that containment vessel strain will be less than 4 percent. The ultimate strain capacity associated with the containment vessel material has been determined to be 22 to 32 percent elongation for ultimate load. Therefore, the results of this assessment showed that the reactor vessel cavity structural concrete may fail locally inside and outside the containment vessel. However, the containment vessel will be less than 20 percent of its ultimate strain capacity, and therefore, the containment vessel will not leak any radioactivity into the atmosphere, and there is no danger due to this postulated steam blast loading. The containment structure can withstand the peak postulated loading from a hinged reactor vessel failure.

B.3.2.2 Reactor Pressure Vessel Response

The vertical uplift of the reactor pressure vessel (RPV) as a result of the steam explosion was assessed, as well as the effects of the RPV motion on the steam generator and attached piping. The worst case loading associated with the hinged reactor vessel failure mode was considered, with the maximum pressure produced by the resulting steam explosion of 24,700 psi (170 Mpa). The total force applied is determined using this pressure and the total area of the RPV based on the reactor pressure vessel outside diameter. The ex-vessel steam explosion is approximated as an impulse load having a peak pressure of 24,700 psi (170 MPa) with a triangular profile of total duration from 0.004 seconds to 0.006 seconds.

The RPV response is evaluated using a one-degree of freedom model. The resulting calculated displacement of the RPV due to the impulse loading is dependent on the system stiffness and mass, with the maximum displacement occurring when the RPV support stiffness approaches zero. This is the case where there is an instantaneous separation of the RPV from the attached piping and no resistance to RPV motion is present. The mass of the RPV used in this evaluation did not include any of the mass associated with the RPV internals since they are considered lost in the steam explosion. Results show that the maximum lift of the RPV (less than 6 feet or about 2 meters) is not sufficient to exceed the height of the walls associated with the biological shield and refueling water canal. Therefore, the RPV motion is contained and will not affect the integrity of the containment structure and associated equipment.

The reactor coolant loop piping deforms plastically with significant RPV uplift due to the steam explosion. Plastic hinges would form in the piping at the biological containment wall penetrations, and at the RPV equipment nozzles, isolating the movement of the RPV from other reactor coolant loop piping and primary components.

The energy released by the worst case ex-vessel steam explosion is insufficient to propel the reactor pressure vessel outside of the walls associated with the biological shield and refueling water canal. The RPV is therefore contained, and will not impact the containment vessel. The effect on other systems and components attached to the loop piping and components is minimized due to the plastic deformation of the loop piping which would isolate the effects of the RPV response due to the ex-vessel steam explosion. The containment vessel will not be compromised as a result of the ex-vessel postulated steam explosion events.

A similar assessment of the potential downward movement of the reactor vessel following an ex-vessel steam explosion in reactor cavity was performed. The downward movement might result from damage to the cavity walls which are part of the reactor vessel support. The assessment concluded that plastic deformation of the loop piping which would isolate the effects of the RPV response. In addition, the potential impact of dropping the reactor vessel onto the cavity floor produces loads that are small compared to the steam explosion loads.

B.4 Core Concrete Interactions

If the reactor vessel fails when the RCS is at a low pressure, the molten core debris will pour from the reactor vessel onto the reactor cavity floor. If a steam explosion does not occur, the pour will spread over the cavity floor and begin to transfer heat to the concrete floor of the reactor cavity. Due to the predicted mode of reactor vessel failure and the shape of the AP600 reactor cavity, analyses of the possible spreading of the core debris over the cavity floor were conducted using the MELTSPREAD code (reference B-6). The results of the MELTSPREAD analyses were then used as input to the MAAP4 code for analysis of core concrete interactions.

An investigation of the spreading of core debris that pours into the reactor cavity was conducted for reactor vessel failure that occurs at low RCS pressure due to the vessel failure mode and location, as well as the recognition that the oxide and metal components of the in-vessel core debris are predicted to be separated. Since the oxide and metal components of the core debris have very different physical characteristics (e.g., viscosity, heat capacity, etc.), the separated in-vessel layers may influence the spreading of the core debris in the reactor cavity. The melt spreading analysis was conducted for both reactor vessel failure modes (hinged and localized failures) using the initial conditions given in Table B-5.

For the hinged vessel failure mode, the entire in-vessel core debris mass was deposited on the cavity floor at a constant rate over a timescale of 10 seconds. The ten second time release period used in this analysis is assumed to be representative of a rapid release in which the metal phase is released distinct from and ahead of the oxide phase. This is roughly equivalent to the assumption that the angle by which the lower head hinges downward increases linearly with time until the head contacts the cavity floor. Because of the assumed rapid hinging failure that conveys the melt largely inside the lower head, no effects of metal water interactions are modelled distinct from normal heat transfer from the melt to the water in the MELTSPREAD code. For the localized failure, a model was developed to calculate the boildown of cavity water level, time dependent melt release rate and melt superheat. This model treated the reactor vessel failure elevation as a function of the cavity water depth (i.e., the failure elevation was maintained just above the cavity water level) by calculating the cavity water boiloff rate as a function of the amount of core debris released to the reactor cavity and the amount of superheat in the core debris. The THIRMAL code was then used to investigate the effects of metal-water interactions upon arrival of materials at the bottom of the pool as the initial portion of the metallic melt relocates downward through the pool. Specifically, the combination of the slow initial release rate and the large water depth would be expected to result in breakup and freezing of the melt as it falls through the water pool, thereby collecting on the cavity floor as a debris bed of solidified particulate. The melt arrival conditions for the MELTSRPEAD analysis were thus based on both calculated release conditions and the THIRMAL results.

The results of the THIRMAL analyses show that most of the core debris (~94 percent) is expected to reach the floor of the cavity in a partially frozen state while the remainder is expected to be fully frozen. None of the initial release of core material from the vessel is

expected to be in a fully molten state. However, as the core debris accumulates on the cavity floor, the decreased water depth will result in an increasing fraction of the core debris arriving in a molten state. The debris arriving in a molten state can fill the interstices and may erode some of the previously solidified debris. Thus, while the initial formation of a porous debris bed cannot be ruled out, the continued addition of molten core material will likely result in a partially frozen debris layer that can further spread over the cavity floor. The results of the THIRMAL analysis were used as the initial conditions for the MELTSPREAD analysis of the localized reactor vessel failure case.

The MELTSPREAD analyses were performed using a reactor cavity model shown in Figure B-3.

For the hinged vessel failure case, the analysis results show that the core debris is spread relatively uniformly over the reactor cavity floor, as shown in Figure B-4. However, the distribution of the metal and oxide components of the core debris are not uniformly distributed over the reactor cavity floor. In the region directly under the reactor vessel, the core debris consists primarily of the oxide component (e.g., 85 to 90 percent oxide). At the opposite end of the reactor cavity, the core debris consists mainly of the metal component of the core debris released from the reactor vessel (e.g., 75 to 85 percent metal). The core debris is still almost totally molten at the end of the spreading analysis. The steel liner over the cavity floor is completely eroded away and the core debris has begun to penetrate into the concrete basemat. The penetration depth at the end of the MELTSPREAD analysis was approximately 1.2 inches (3 cm) under the reactor vessel and about 2.75 inches (7 cm) at the opposite end of the reactor cavity.

A different behavior is predicted for the localized reactor vessel failure case. The MELTSPREAD analysis predicts that the core debris will accumulate at the reactor vessel end of the reactor cavity as shown in Figure B-5. The distribution of the metal and oxide components of the core debris are not uniformly distributed over the reactor cavity floor. In the region directly under the reactor vessel, the core debris consists primarily of the oxide component (e.g., 70 to 80 percent oxide). At the opposite end of the reactor cavity, the core debris consists mainly of the metal component of the core debris released from the reactor vessel (e.g., 80 to 90 percent metal). The core debris is almost totally frozen at the end of the spreading analysis. The steel liner over the cavity floor is not eroded (except for one node of the cavity model under the reactor vessel) and the core debris has only begun to penetrate the concrete basemat in one node.

The results of the MELTSRPEAD analyses were used to establish initial conditions for assessment of core concrete interactions using the MAAP4 code models. Since MAAP4 can only treat the core debris that is uniformly spread over a cavity floor, two parallel MAAP4 analyses were done for each vessel failure mode. The first analysis for each vessel failure mode treats the core debris under the reactor vessel while the second analysis treats the core debris that is in the reactor coolant drain tank (RCDT) end of the cavity. In all cases, the results of the MELTSPREAD analysis were used to define the initial conditions for the core concrete interactions using the MAAP4 models. Since one portion of the reactor cavity

initially contains oxide-rich core debris and the other end contains metal-rich core debris, the rate of concrete decomposition is controlled by different factors in each analysis. The oxide-rich debris contains most of the fission product decay heat and this controls the concrete decomposition. The metal-rich debris does not contain decay heat but is subject to exothermic heat of reaction of steam with the unoxidized metal and this controls the concrete decomposition.

For the hinged reactor vessel failure case, the core concrete interaction analysis shows (see Figures B-6a and B-6b) that the concrete basemat in the region of the cavity under the reactor vessel is eroded much more rapidly than the region of the RCDT. At 24 hours (8.64E4 seconds) into the accident, the downward erosion is almost 3.9 feet (1.2 meters) on the reactor vessel side of the cavity while the erosion is only about 1.15 feet (0.35 meters) on the RCDT side. The core debris depth on reactor vessel side (including the decomposed concrete products) measures about 3.6 feet (1.1 meters). Thus, while the containment shell is only 2.3 feet (0.7 meters) from original cavity floor and would be penetrated by the leading edge of the core debris, the containment shell would still be covered by a substantial layer of core debris and would not communicate with the containment atmosphere for passable fission product releases at 24 hours. The leading edge of the core debris is predicted to penetrate the containment shell that is buried in the basemat at about 32000 seconds or about 9 hours after the accident initiation.

For the case of the localized reactor vessel failure, the core concrete interaction analysis also shows (see Figures B-7a and B-7b) that the concrete basemat in the region of the cavity under the reactor vessel is eroded much more rapidly than the region of the RCDT. At 24 hours (8.64E4 seconds) into the accident, the downward erosion is almost 3.9 feet, or 1.2 meters, (almost identical to the hinged vessel failure case) on the reactor vessel side of the cavity while the erosion is only about 1.0 foot (0.31 meters) on the RCDT side. The core debris depth on reactor vessel side (including the decomposed concrete products) measures about 3.3 feet (1.0 meters). Thus, while the containment shell is only 2.3 feet (0.7 meters) from original cavity floor and would be penetrated by the leading edge of the core debris, the containment shell would still be covered by a substantial layer of core debris and would not communicate with the containment atmosphere for possible fission product releases at 24 hours. The leading edge of the core debris is predicted to penetrate the containment shell that is buried in the basemat at about 37000 seconds or at a little over 10 hours after the accident initiation.

B.4.1 Containment Pressurization Due to Core Concrete Interactions

The containment pressurization due to steam and noncondensible gas generation during the episodes of core concrete interactions described above was assessed to determine the effect of core concrete interactions on the containment integrity.

To estimate the effect of steam and noncondensible gas generation on the containment pressure and temperature, the AP600 containment was included in the separate effects MAAP4 analysis of core concrete interactions described above. Since the core concrete interaction

assessment with MAAP4 was a "separate effects" analysis, the initial containment conditions were specified to be 21.8 psia (0.15 MPa) at saturation conditions represented by a steam-air mixture. The MAAP4 analysis results are very similar for both reactor vessel failure modes described above. In both cases the containment conditions at the end of one day, as predicted by the MAAP4 code, show a containment pressure of 40 psia (0.275 MPa) and a containment temperature of 305°F (425°K).

From these results, it is concluded that the containment conditions at 24 hours after reactor vessel failure are not sensitive to the assumed mode of reactor vessel failure. In both cases, the containment pressurizes by about 14.5 psi (0.1 MPa) in 24 hours due to the steam and noncondensible gases generated during core concrete interactions.

A separate bounding calculation was also performed in which all of the gases from the core concrete interaction, as predicted by the MAAP4 analyses described above, were assumed to be released to the containment with no condensation of the steam that is generated from the concrete decomposition. In this case, it is calculated that the containment would pressurize by 21.8 psi (0.15 MPa) in 24 hours.

In both the MAAP4 and the bounding calculations, the containment pressure is still well below the point where the integrity of the containment might be challenged.

B.5 Conclusions

The results of the limited deterministic analyses of ex-vessel severe accident phenomena presented in this section show that early containment failure is not a certainty if the reactor vessel fails. Based on the deterministic analyses, direct containment heating that might ensue from a high pressure melt ejection would not challenge the integrity of the containment. Ex-vessel steam explosions, assessed on a very conservative basis would not produce impulse loads that would challenge the integrity of the containment due to localized failures of the reactor cavity floor and walls. In addition, these analyses indicate that the ex-vessel steam explosion loads are not strong enough to displace the reactor vessel from its location inside the biological shield. Thus, there is no challenge to any containment penetrations connected to the reactor vessel or to the reactor coolant loops. In the case of a vessel failure at a low RCS pressure, the core concrete interactions analyses indicate that the containment integrity would not be challenged in the first 24 hours of the event and thus no significant releases of fission products are predicted in that time frame.

Thus, it is concluded that prevention of large fission product releases to the environment is not dependent on the integrity of the reactor vessel. If reactor vessel failure occurs, there may be challenges to the containment integrity, but these challenges are highly uncertain and the most likely challenge (containment failure by core penetration of the cavity basemat) would not occur in the first 24 hours of the accident. Thus, the AP600 assumption that reactor vessel failure always leads to containment failure is a conservatism in the AP600 risk profile.

B.6 References

B-1 "AP600 Phenomenological Evaluation Summaries," WCAP-13388 (Proprietary) Rev. 0, June 1992 and WCAP-13389 (Nonproprietary), Rev. 1, 1994.

B-2 Theofanous, T.G., et al., "In-Vessel Coolability and Retention of a Core Melt," DOE/ID-10460, July 1995.

B-3 "The Influence of Selected Containment Structures on Debris Dispersal and Transport Following High Pressure Melt Ejection From the Reactor Vessel," NUREG/CR-4914, September 1988.

B-4 Pilch, M.M., "Adiabatic Equilibrium Models For Direct Containment Heating," SAND-91-2407C, December 1992.

B-5 "Code Manual for Texas-IV: One Dimensional Transient Fluid Model Fuel Coolant Interaction Analysis," Corradini, et al., Univ of Wisconsin, October 1994.

B-6 Sienicki, J.J., et al., "Analysis of Melt Spreading in an AP600-Like Cavity," DOE/ID-10523, February 1996.

Table B-1

CHARACTERISTICS OF CORE DEBRIS INSIDE REACTOR VESSEL AT VESSEL FAILURE

Parameter	Value
Melt Mass Inside Lower Head, Kg	
UO_2	75,900
ZrO_2	8,500
Stainless Steel	70,000
Zr	12,900
Melt Configuration Inside Lower Head	Metal Layer Overlying Oxide Pool
Depth of oxide Inside Lower Head, meters	1.48
Thickness of Metal Layer Inside Lower Head, meters	0.94
Initial Water Level Above Cavity Floor, meters	3.89
Initial Cavity Water Volume, $meters^3$	193
Time of Vessel Failure after Reactor Trip, seconds	11,800

(from reference B-6)

Table B-2

MAJOR INPUT PARAMETERS FOR THE PILCH 2-CELL DCH MODEL

Parameter	Value
Volume of SG Compartments (Cell #1), $meter^3$	7099.18
Volume of Upper Containment (Cell #2), $meter^3$	40265.5
Flow Area of Tunnel From Cavity to SG Compartments, $meter^2$	3.5052
Flow Area Through Loop Nozzle Penetrations, $meter^2$	16.1544
Flow Area past RV Flange, $meter^2$	2.1082
Mass of UO2 in the Core, kg	75900
Mass of Zr in the Core, kg	19200
Fraction of Core Mass Ejected from Reactor Vessel	0.5
Fraction of Core Mass Ejected from Reactor Cavity	1.0
Initial Containment Pressure, MPa	0.31
Initial Containment Relative Humidity	1.0
Temperature of Ejected Core Debris,°K	2478
Fraction of Ejected Zirc Unoxidized	0.5
RCS Pressure at Vessel Failure, MPa	15.17
RCS Gas Temperature at Vessel Failure,°K	925

Table B-3

MAJOR INPUT PARAMETERS FOR THE TEXAS EX-VESSEL STEAM EXPLOSION ANALYSES

Parameter	Vessel Failure Mode	
	Hinged	**Localized**
Melt Flow Rate, kg/s	15,100	3.8
Melt Superheat, °K	80	80
Melt Temperature, °K	1890	1890
Melt Density, kg/m^3	7800	7800
Coherent Jet Diameter, meters	0.068	0.060
Number of Coherent Jets	236	1
Jet Velocity, m/s	2.26	0.17
Nominal Pool Area, m^2	20	2.5

Table B-4

SENSITIVITY ANALYSES USING THE TEXAS EX-VESSEL STEAM EXPLOSION MODELS

Parameter	Parameter Value		Impact on Impulse Loading
	Base Case	Sensitivity Case	
Melt Superheat,°K	80	100	+ 4%
Water Pool Area, m^2	2.5	5	- 30%
Breakup Model	Trailing Edge	Leading Edge	~ 0
Water Pool Temperature,°K	342	385	+ 25%

Table B-5

MAJOR INPUT PARAMETERS FOR THE MELTSPREAD EX-VESSEL CORE DEBRIS SPREADING ANALYSES

Parameter	Vessel Failure Mode
Melt Mass Inside the Lower Head, kg	
UO_2	75,900
ZrO_2	8,500
Stainless Steel	70,000
Zr	12,900
Melt Configuration Inside the Lower Head	Metal Layer Overlying Oxide Pool
Time of Vessel Failure, seconds	11,800
Cavity Floor Area, m^2	22
Reactor Coolant Drain Tank compartment Floor Area, m^2	26
Total Cavity Floor Area, m^2	48
Initial Water Level Above Cavity Floor, meters	3.89

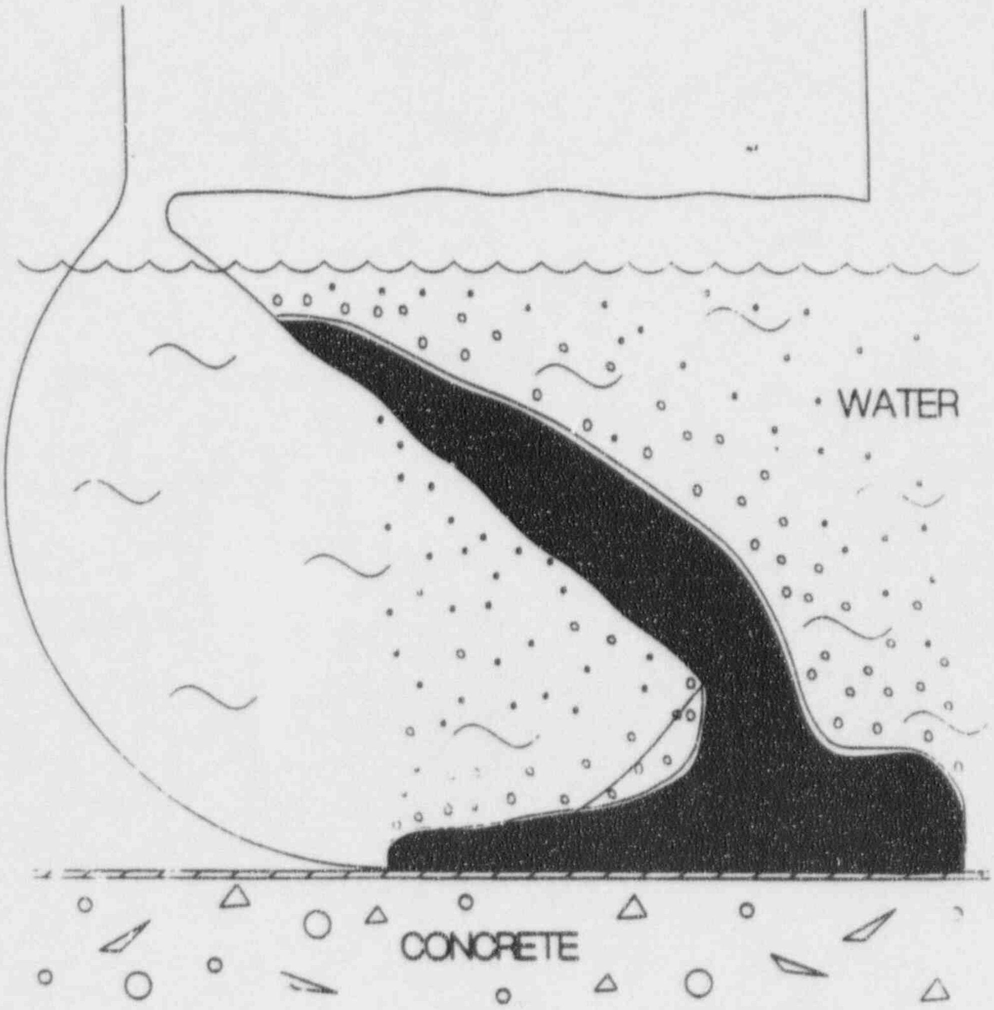

Figure B-1

Illustration of Hinging Type of Failure Resulting in Rapid Melt Release (from Reference B-6)

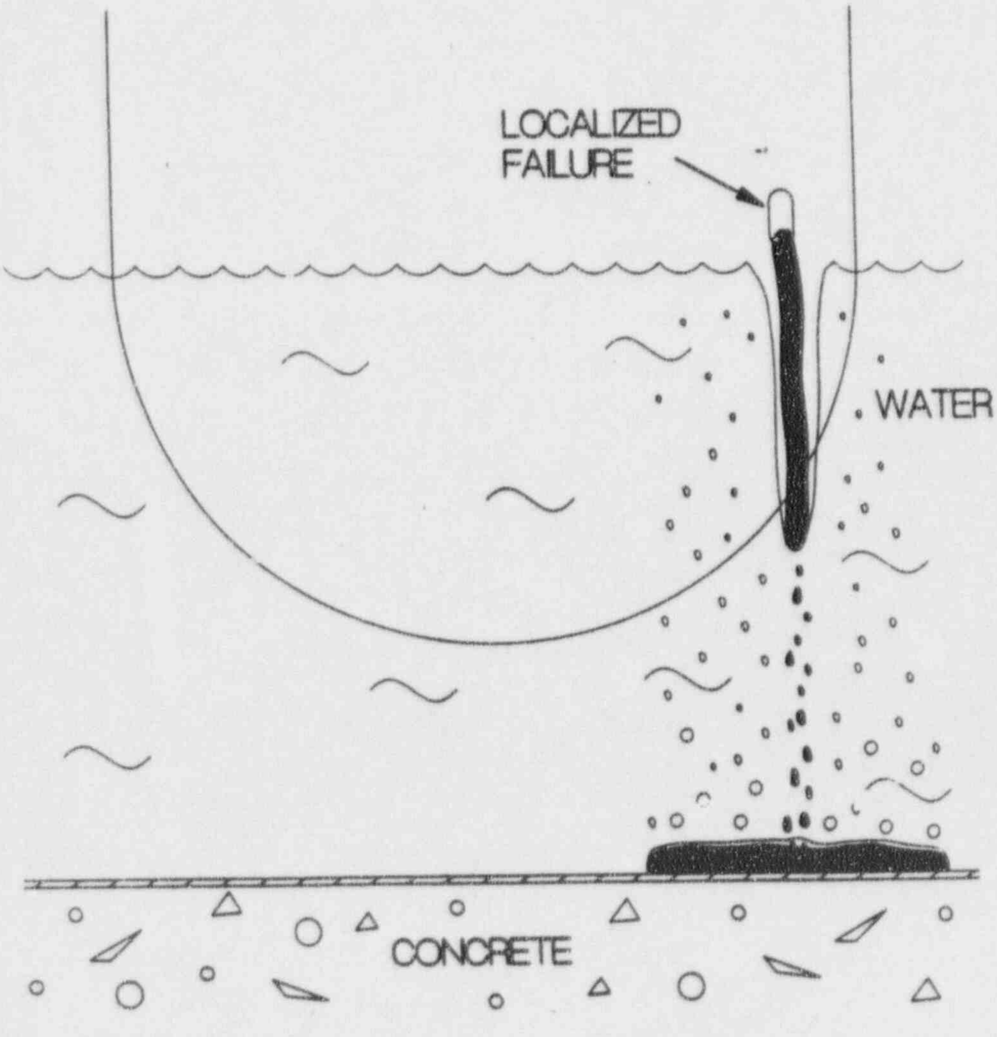

Figure B-2

Illustration of Localized Type of Failure Resulting in Slow Melt Release (from Reference B-6)

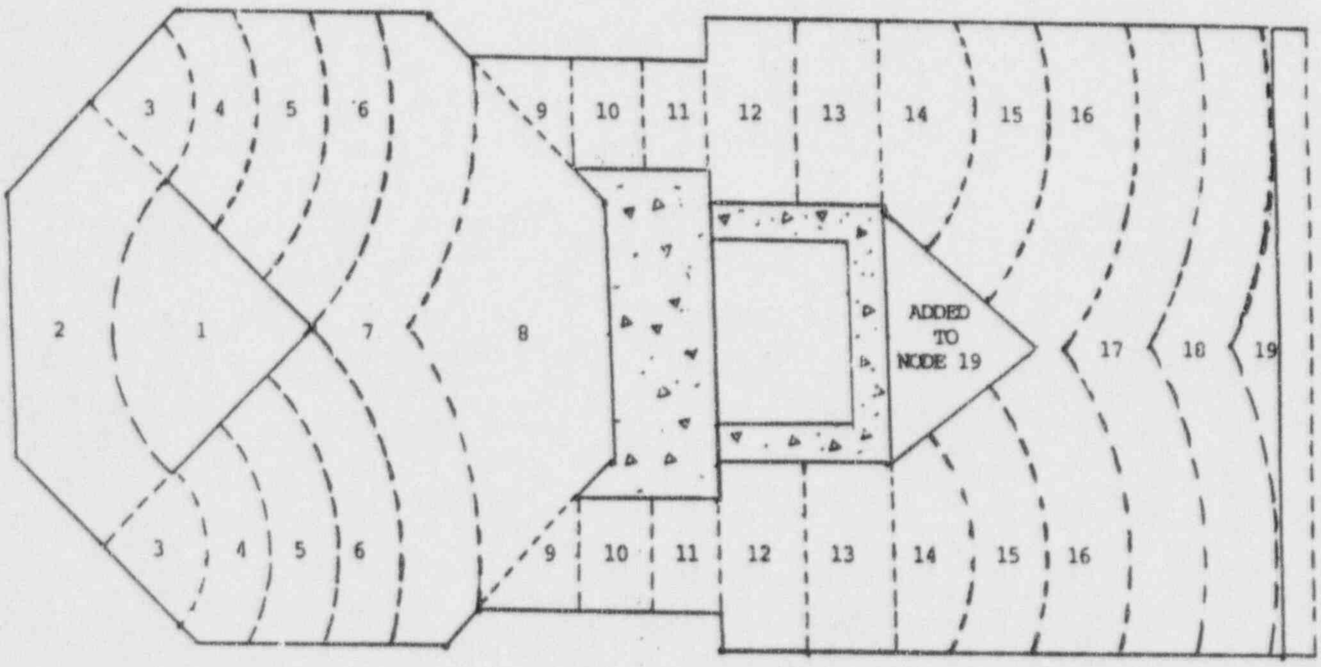

Figure B-3

Nodalization of Cavity, Personnel Access, Ventilation Duct, and Reactor Coolant Drain Tank (RCDT) (from Reference B-6)

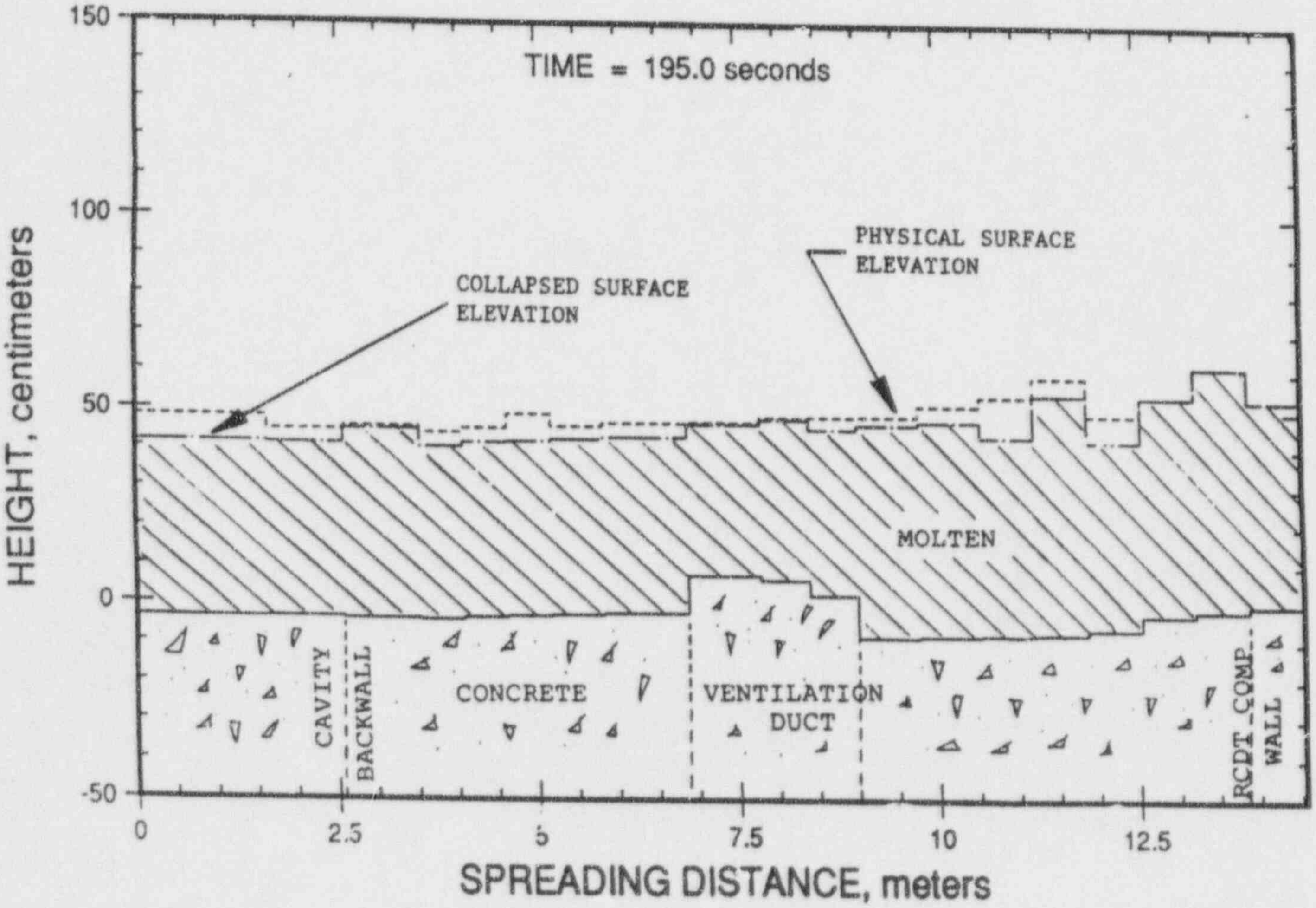

Figure B-4

Scenario I Melt Spreading and Floor Surface Elevation Distribution at 195 Seconds (from Reference B-6)

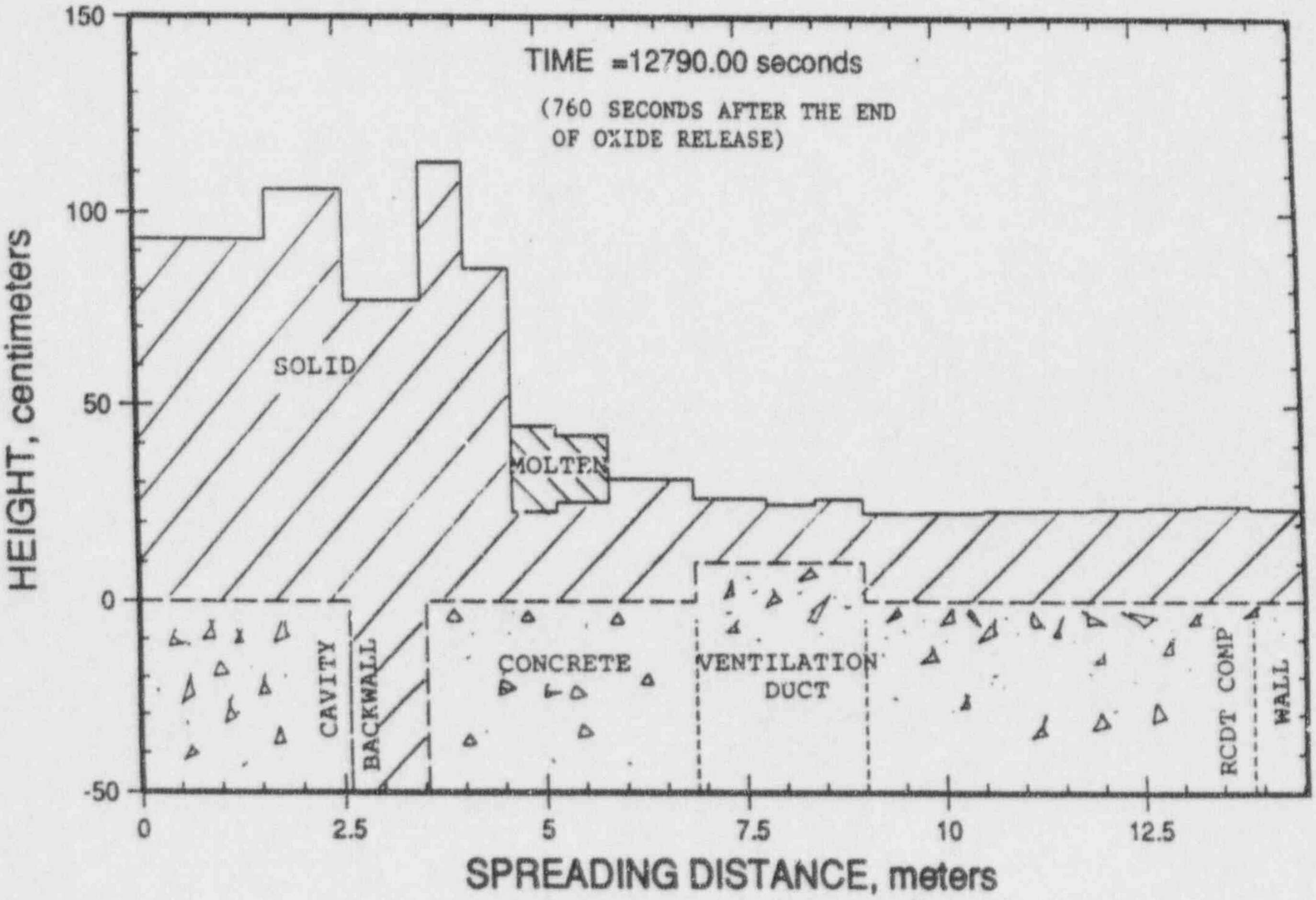

Figure B-5

Scenario II Melt Spreading and Floor Surface Elevation Profiles at 12790 Seconds (from Reference B-6)

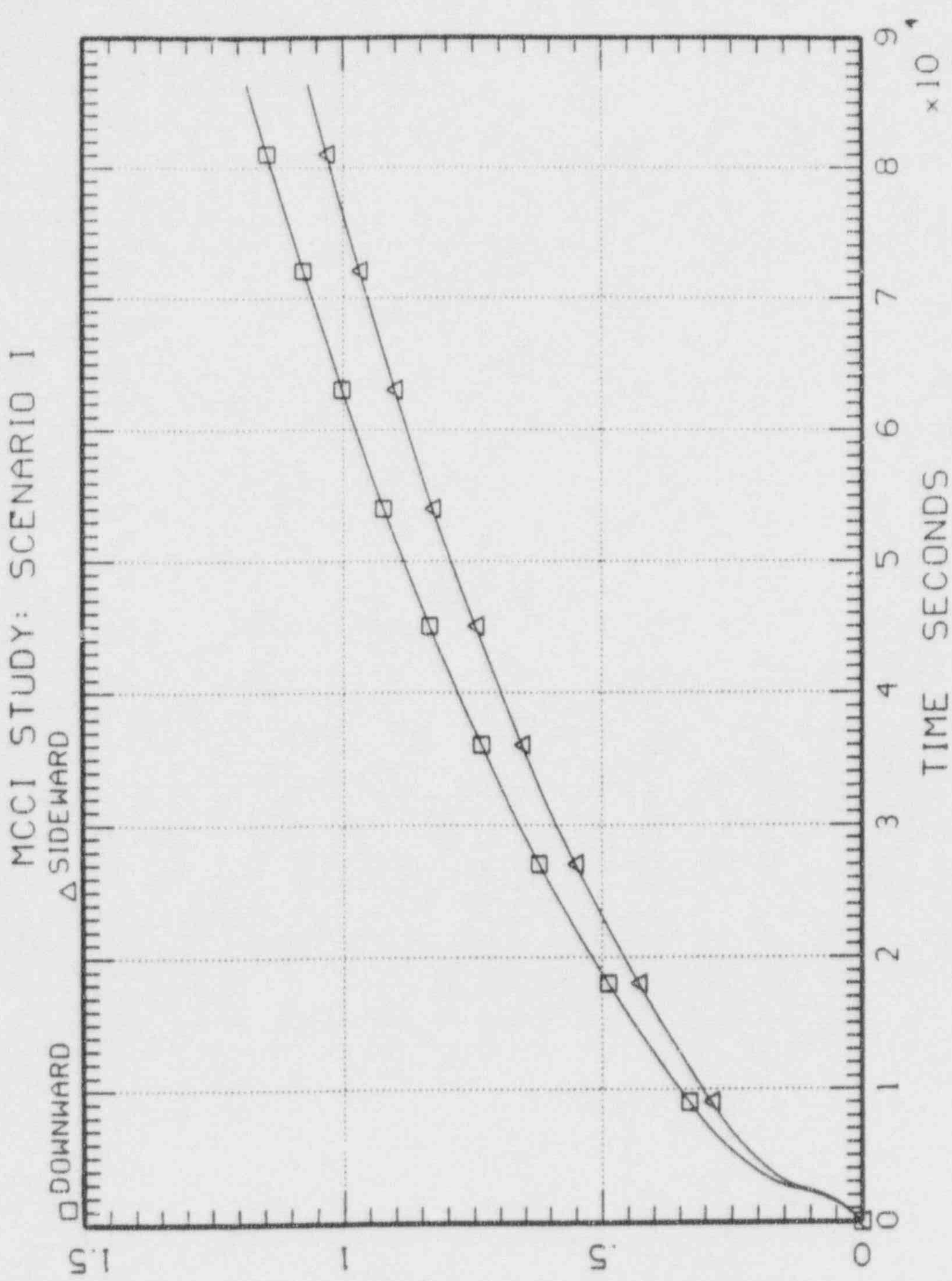

Figure B-6a

Scenario I: RC Ablation

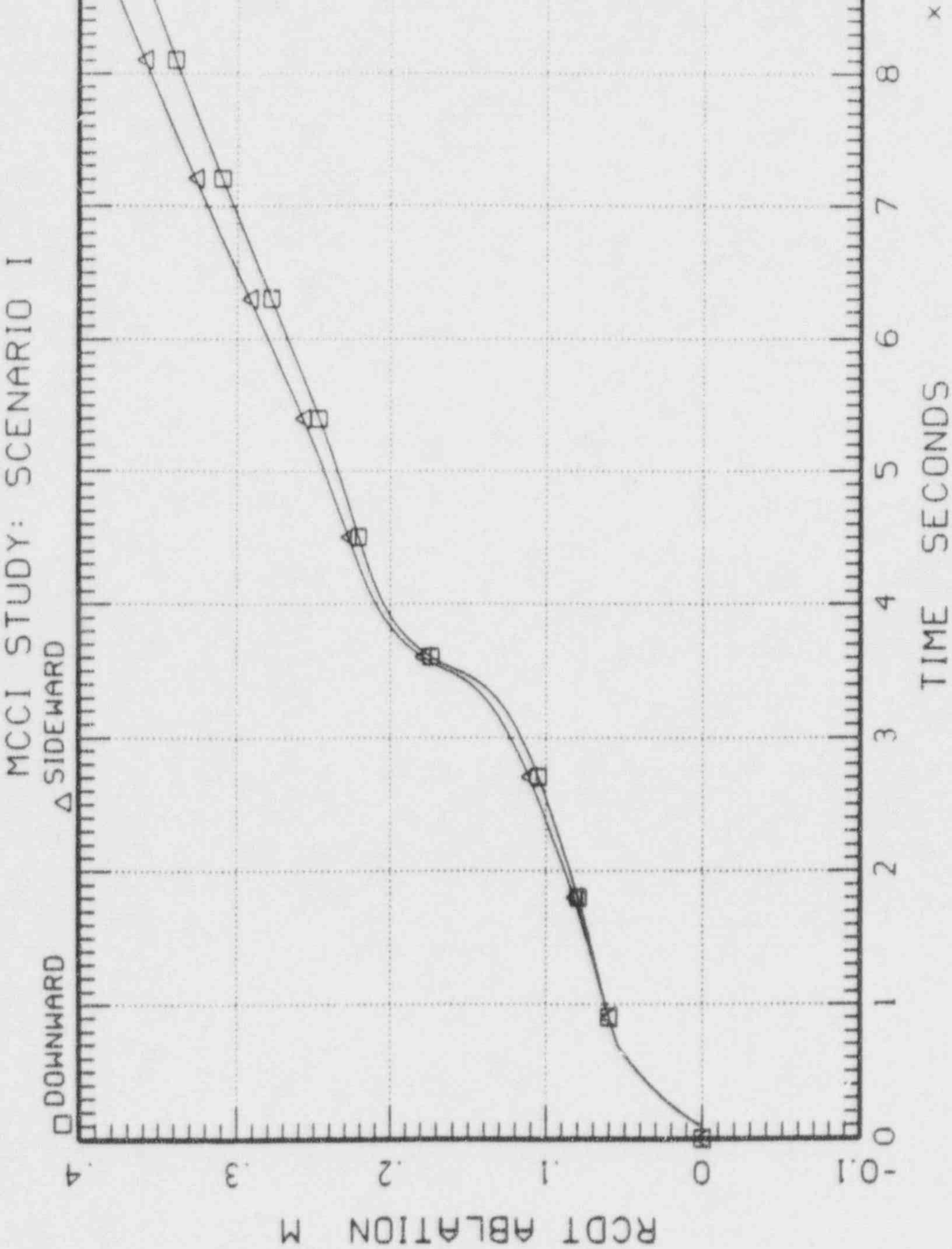

Figure B-6b

Scenario I: RCDT Ablation

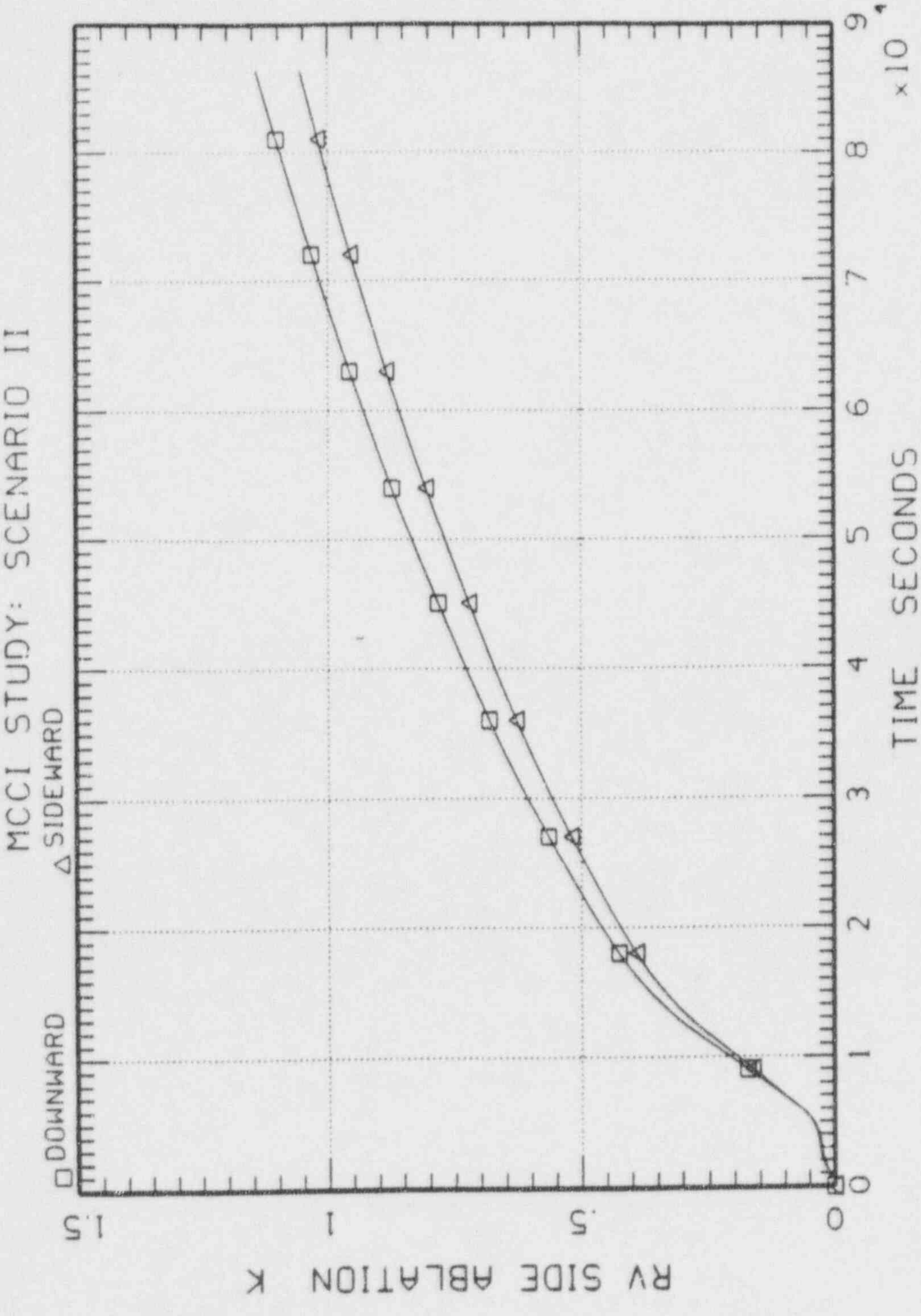

Figure B-7a

Scenario II: RC Ablation

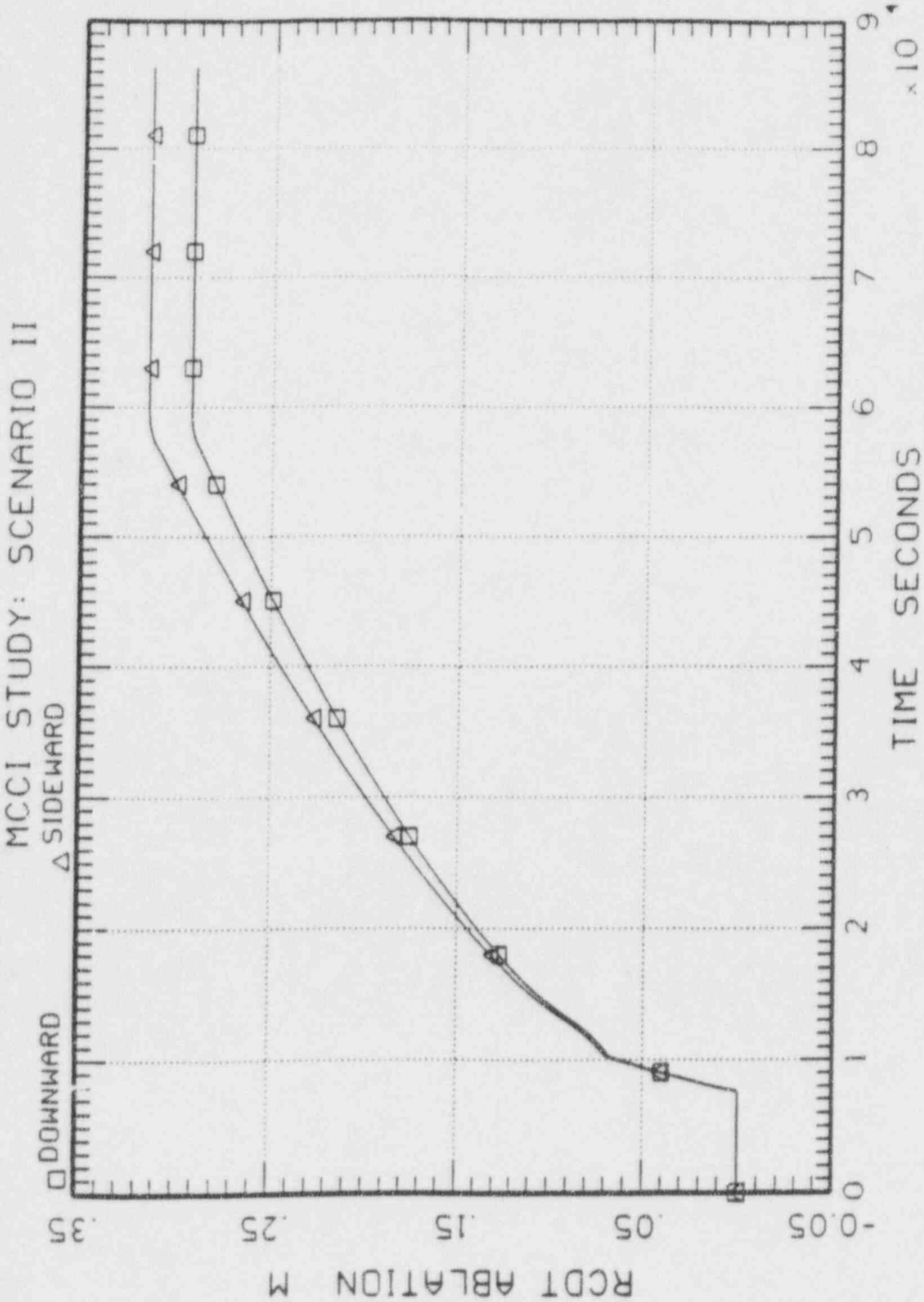

Figure B-7b

Scenario II: RCDT Ablation